Int. J. Solids Structures Vol. 30, No. 15, pp. 2117–2139, 1993
Printed in Great Britain

0020–7683/93 $6.00+ .00

INTERACTION OF PENNY-SHAPED CRACKS WITH A HALF-PLANE CRACK

X. HUANG and B. L. KARIHALOO†
School of Civil and Mining Engineering, The University of Sydney, NSW 2006, Australia

(*Received* 6 *February* 1992; *in revised form* 18 *January* 1993)

Abstract—Three-dimensional interactions between a half-plane crack and penny-shaped cracks which are not necessarily located in the same plane are analysed using the "weight function" method of three-dimensional crack analysis. Analytical expressions are given for the interaction kernels in the integral equations with the opening displacements of penny-shaped cracks as unknown functions. By using the Rayleigh–Ritz method the singularities of the kernels are weakened to make them suitable for finite element calculations. The weak form equations are also solved by a simple method after approximating the opening displacement over each crack by a constant times a square root function of the distance from its edge. This simple method of solution is shown to give results which are in excellent agreement with those of Laures and Kachanov (1991, *Int. J. Fract.* **48**, 255–279).

1. INTRODUCTION

Two-dimensional macro-microcrack interaction has been discussed by several authors, because of its importance as a potential shielding mechanism. There are various analytical methods for investigating this class of problems [see for example Rose (1986), Rubinstein (1986), Gong and Horii (1989) and Shum and Hutchinson (1990)].

Of particular interest is the method of pseudo-tractions proposed by Horii and Nemat-Nasser (1985) in which the original problem is decomposed into several subproblems, each containing just one crack. The stress field and the stress intensity factors at the various crack tips are found by summing the stress intensity factor or the stress field contributions from each of the subproblems. In the actual analysis of each subproblem crack face force doublets are chosen as unknowns which are determined from the traction-free condition on crack faces. The satisfaction of the traction-free condition on each of the cracks results in a system of singular integral equations. Various numerical procedures have been proposed to solve this system of integral equations.

The present paper is concerned with the three-dimensional counterpart of the above problems. Specifically, the paper considers the interaction between a half-plane crack and finite cracks which are not necessarily located in the same plane. The original problem is decomposed into several subproblems each containing the half-plane crack and one of the cracks of the original problem. The crack opening displacement is used as the unknown function in the three-dimensional problem because of its known behaviour near the crack edge. It can therefore be accurately approximated in terms of this known behaviour and piece-wise linear functions. Such an approach has been previously taken by Huang and Karihaloo (1992) in the study of interaction of penny-shaped cracks.

The use of the three-dimensional weight functions (Rice, 1985; Bueckner, 1987; Karihaloo and Huang, 1989) permits the introduction of kernel functions in the integral equations which depend only on the half-plane crack but are otherwise independent of the shape and distribution of the other cracks. This allows the determination of kernel functions analytically or numerically with integrations extending only over finite domains. By using the Rayleigh–Ritz method, the strong singularity in the weight functions can be replaced by a weak one suitable for finite element approximation to the finite domain. The finite element method provides a reliable solution even when the cracks are very close to each other. Additionally, a simple approximate solution is obtained by replacing the opening displacement of each penny-shaped crack by a constant times a square-root function of the

† Current address: Institute of Mechanics, Aalborg University, Pontoppidanstraede 101, DK 9220 Aalborg East, Denmark.

distance from the edge. This approximation is shown to give the same results as that of Laures and Kachanov (1991) who regarded the (constant) average traction over the crack faces as the unknown in their study of the macro–microcrack interaction. When the distance between the cracks increases the approximate solutions tend to the finite element solutions.

2. MATHEMATICAL FORMULATION

Consider a half-plane crack (labelled B in Fig. 1) in an infinite elastic space. The crack lies in the plane $y = 0$ and its front is parallel to the z-axis along $x = a$, such that the region $x < a$ is cracked. As is well known, in the absence of any other cracks arbitrary applied loadings characterized by stress intensity factors K_α^∞ induce singular stress fields σ_{ij}^∞ $(i, j = x, y, z)$ ahead of the front

$$\sigma_{ij}^\infty = K_\alpha^\infty \tilde{\sigma}_{ij}^\alpha(\phi)/\sqrt{2\pi\rho}, \tag{1}$$

where $\alpha = \mathrm{I}, \mathrm{II}, \mathrm{III}$ stand for the three different modes of loading, $\tilde{\sigma}_{ij}^\alpha(\phi)$ depend only on ϕ, and (ρ, ϕ) are polar coordinates in the plane $(x-a, y)$.

Consider next a group of cracks of finite length denoted as A_i $(i = 1, \ldots, n)$ interacting with the above half-plane crack and with each other. The displacement discontinuity over a generic crack A_i from this group is denoted by T_k^i $(k = x, y, z)$. Let the altered stress intensity factor along the front of the half-plane crack be denoted by K_α. The position of crack A_i is described by the position vector of its geometric centre $\mathbf{r}_0$ and by the outward normal $\mathbf{n} = (n_1, n_2, n_3)$. From dimensional considerations and the fact that a linear problem is being analysed, it may be concluded that

$$K_\alpha/K_\alpha^\infty = \mathscr{F}(\mathbf{r}_0/b_i, \mathbf{n}), \tag{2}$$

where b_i denotes the characteristic size of A_i. To gain an insight into the interaction problem, the mathematical formulation will be illustrated on specific examples. The formulation however provides a good basis for the most general interaction problem, when the finite cracks are arbitrarily distributed. Likewise, the choice of penny-shaped cracks should not prove restrictive because the finite element technique used to solve the problem numerically is applicable to any regular shaped cracks.

2.1. *Two coplanar penny-shaped cracks ahead of a half-plane crack*

Consider two penny-shaped cracks of identical radius b ahead of the half-plane crack. The cracks are located symmetrically with respect to $z = 0$ in the plane $y = 0$. Denote the

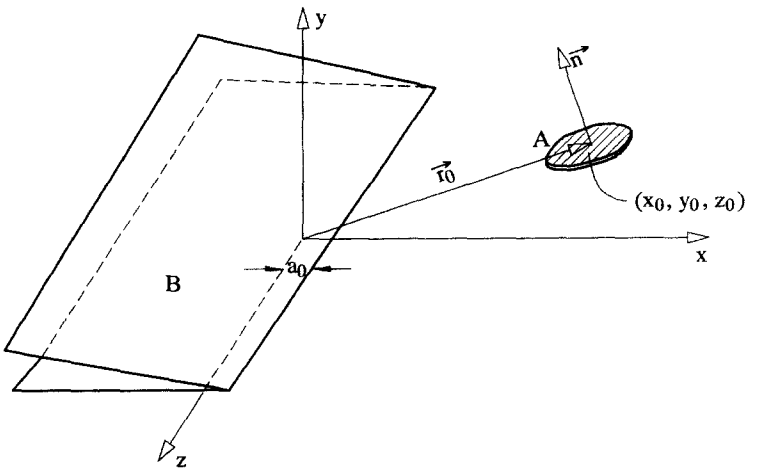

Fig. 1. A half-plane crack (B) and an arbitrarily located and oriented penny-shaped crack (A).

cracks by A^1 and A^2 and let the distance between their centres be d, such that $d > 2b$. The cracks are assumed to be entirely in the region $x > a$, so that they never come in contact with the half-plane crack. The external loading is assumed to have mode I symmetry, so that the only nonvanishing component of displacement discontinuity on A^t ($t = 1, 2$) is the y-direction opening displacement $T_y^t(x, 0, z)$. For brevity, the subscript will be omitted in the sequel. By symmetry, $T^1(x, 0, z) = T^2(x, 0, -z) \equiv T(x, z)$, so that we need to find just one unknown displacement discontinuity. The original problem is regarded as the superposition of three subproblems. The first subproblem represents the half-plane crack subjected to the applied stress intensity factor K_I^∞. Each of the remaining subproblems contains just one penny crack which is subjected to unknown pseudo-tractions from the remaining crack in the presence of the half-plane crack. The stress intensity factor $K_I(z', a)$ induced along the half-plane crack front by the external loading in the presence of the two penny cracks can be evaluated as

$$K_I(z', a) = K_I^\infty(z', a) + K_I^{BA^1}(z', a) + K_I^{BA^2}(z', a). \tag{3}$$

The stress intensity factor $K_I^{BA^t}$ induced at location z' along crack front $x = a$ by a distribution of displacement discontinuities T^t over A^t is (Rice, 1985)

$$K_I^{BA^t}(z', a) = (\lambda + 2\mu) \int\int_{A^t} h_{1y,y}(x, 0, z; z', a) T^t(x, 0, z)\, dx\, dz$$

$$= \frac{\mu}{(2\pi)^{3/2}(1-\nu)} \int\int_{A^t} \frac{T^t(x, 0, z)}{\sqrt{x-a}[(x-a)^2 + (z-z')^2]}\, dx\, dz, \tag{4}$$

where the function $h_{1y,y}(x, 0, z; z', a)$ was obtained by Rice (1985). Here and in the sequel the integral is taken over one of the two plane crack surfaces, designated A^t for brevity. The unknown opening displacement $T^t(x, 0, z)$ is obtained from the traction-free condition on the penny crack (no summation over repeated y)

$$\sigma_{yy}(\mathbf{r}) n_y = 0, \tag{5}$$

where $n_y = 1$, and

$$\sigma_{yy}(\mathbf{r}) = \sigma_{yy}^\infty(\mathbf{r}) + [\sigma_{yy}^{A^1}(\mathbf{r}) + \sigma_{yy}^{BA^1}(\mathbf{r})] + [\sigma_{yy}^{A^2}(\mathbf{r}) + \sigma_{yy}^{BA^2}(\mathbf{r})]. \tag{6}$$

The superscripts designate the sources of contribution. In the present special case, the interaction stress field can be represented as (Rice, 1985):

$$\sigma_{yy}^{BA^t}(\mathbf{r}) = 8\mu^2 \int\int_{A^t} T^t(\tilde{x}, 0, \tilde{z}) H(\mathbf{r}, \tilde{\mathbf{r}})\, d\tilde{x}\, d\tilde{z}$$

$$= \frac{\mu}{2\pi^2(1-\nu)} \int\int_{A^t} \frac{1}{R^3} \left[\frac{R}{2(x\tilde{x})^{1/2}} - \arctan \frac{R}{2(x\tilde{x})^{1/2}} \right] T^t(\tilde{x}, 0, \tilde{z})\, d\tilde{x}\, d\tilde{z}, \tag{7}$$

where the general expression for $H(\mathbf{r}, \mathbf{r})$ is given in Appendix A. Following Bui (1977), Kupradze (1963) and Cruse (1969), it may be shown by the use of the potential theory for single and double layers that

$$\sigma_{yy}^{A^t}(\mathbf{r}) = \frac{\mu(1-2\nu)}{2\pi(1-\nu)} \int\int_{A^t} \frac{1}{R^3} T^t(\tilde{\mathbf{r}})\, d\tilde{x}\, d\tilde{z} \quad (\mathbf{r} \notin A^t),$$

$$\sigma_{yy}^{A^t}(\mathbf{r}) = -\frac{\mu}{4\pi(1-\nu)} \int\int_{A^t} \left[\left(\frac{1}{R}\right)_{,\tilde{x}} T_{\tilde{x}}^t + \left(\frac{1}{R}\right)_{,\tilde{z}} T_{\tilde{z}}^t \right] d\tilde{x}\, d\tilde{z} \quad (\mathbf{r} \in A^t). \tag{8}$$

In the second equation, $\mathbf{r}$ must be on A^t for a fixed t. The traction-free condition on A^1 or A^2 gives the following singular integral equation for the determination of $T^1(x,0,z)$, and by symmetry, that of $T^2(x,0,-z)$:

$$-\frac{\mu}{4\pi(1-\nu)}\iint_A\left[\left(\frac{1}{R}\right)_{,\tilde{x}}T_{,\tilde{x}}(\tilde{x},\tilde{z})+\left(\frac{1}{R}\right)_{,\tilde{z}}T_{,\tilde{z}}(\tilde{x},\tilde{z})\right]d\tilde{x}\,d\tilde{z}$$
$$+\frac{\mu(1-2\nu)}{2\pi(1-\nu)}\iint_A\frac{T(\tilde{x},\tilde{z})}{R^3(-\tilde{z})}d\tilde{x}\,d\tilde{z}+\frac{K_1^\infty}{\sqrt{2\pi(x-a)}}$$
$$+\frac{\mu}{2\pi^2(1-\nu)}\iint_A\frac{1}{R^3}\left[\frac{R}{2(x\tilde{x})^{1/2}}-\arctan\frac{R}{2(x\tilde{x})^{1/2}}\right]T(\tilde{x},\tilde{z})\,d\tilde{x}\,d\tilde{z}$$
$$+\frac{\mu}{2\pi^2(1-\nu)}\iint_A\frac{1}{R^3(-\tilde{z})}\left[\frac{R(-\tilde{z})}{2(x\tilde{x})^{1/2}}-\arctan\frac{R(-\tilde{z})}{2(x\tilde{x})^{1/2}}\right]T(\tilde{x},\tilde{z})\,d\tilde{x}\,d\tilde{z}=0, \tag{9}$$

where $R(-\tilde{z})=[(x-\tilde{x})^2+(z+\tilde{z})^2]^{1/2}$.

The singular integral equation (9) may be solved in a variety of ways. Here we use the finite element method. By using the Rayleigh–Ritz method, the singularity of the integral equation can be weakened, as follows. Denote by $B(T,T')$ the bilinear form:

$$B(T,T')=\frac{\mu}{4\pi(1-\nu)}\iint_A dx\,dz\iint_A\left\{\frac{1}{R}[T'_{,x}(x,z)T_{,\tilde{x}}(\tilde{x},\tilde{z})+T'_{,z}(x,z)T_{,\tilde{z}}(\tilde{x},\tilde{z})]\right.$$
$$\left.-q(x,z,\tilde{x},\tilde{z})T'(x,z)\,T(\tilde{x},\tilde{z})\right\}d\tilde{x}\,d\tilde{z} \tag{10}$$

where

$$q(x,z,\tilde{x},\tilde{z})=\frac{\mu(1-2\nu)}{2\pi(1-\nu)}\frac{1}{R^3(-\tilde{z})}+\frac{\mu}{2\pi^2(1-\nu)}\frac{1}{R^3}\left[\frac{R}{2(x\tilde{x})^{1/2}}-\arctan\frac{R}{2(x\tilde{x})^{1/2}}\right]$$
$$+\frac{\mu}{2\pi^2(1-\nu)}\frac{1}{R^3(-\tilde{z})}\left[\frac{R(-\tilde{z})}{2(x\tilde{x})^{1/2}}-\arctan\frac{R(-\tilde{z})}{2(x\tilde{x})^{1/2}}\right]. \tag{11}$$

Let

$$f(\mathbf{r})=\frac{K_1^\infty}{\sqrt{2\pi(x-a)}} \tag{12}$$

and define the inner product

$$(f,T')=\iint_A f(x,z)T'(x,z)\,dx\,dz. \tag{13}$$

Let T and T' be two crack opening displacements of A^1 or A^2. The weak form of the singular integral equation (9) suitable for finite element approximation is derived as follows. Multiply both sides of (9) by $T'(x,z)$ and integrate over the domain A^1 or A^2. The reciprocal relation yields the weak form of (9), namely

$$B(T,T')=(f,T'). \tag{14}$$

It is obvious from (10) that the bilinear form is symmetric

$$B(T,T')=B(T',T). \tag{15}$$

Futhermore, $B(T, T) > 0$, since by (14) it is equal to the work done by the pressure $f(\mathbf{r})$ in opening the penny crack in the presence of a half-plane crack. It follows that the variational problem for the functional

$$J(T) = \tfrac{1}{2}B(T, T) - (f, T) \tag{16}$$

will lead to the unique solution of (14).

We also list the bilinear form for the case of a single penny crack in the plane $y = 0$. Instead of (11), we have

$$q(\mathbf{r}, \tilde{\mathbf{r}}) = \frac{\mu}{2\pi^2(1-\nu)R^3}\left[\frac{R}{2(x\tilde{x})^{1/2}} - \arctan\frac{R}{2(x\tilde{x})^{1/2}}\right] \tag{17}$$

which together with (10) gives the required bilinear form.

2.2. *Two parallel and symmetrically located penny cracks*

Consider two penny-shaped cracks of equal size symmetrically located with respect to $y = 0$, a distance d apart. Denote these cracks A^1 and A^2. Assume, as before, that the external loading has mode I symmetry, so that the major nonzero components of displacement discontinuity on A^1 and A^2 are T^1 and T^2, respectively. By symmetry, $T^1(x, d/2, z) = T^2(x, -d/2, z) \equiv T(x, z)$. Again, the subscript y has been omitted. The stress intensity factor $K_I(z', a)$ induced along the front of the half-plane crack by the opening displacements of the penny cracks can be evaluated by superposition

$$K_I = K_I^{\infty} + K_I^{BA^1} + K_I^{BA^2}, \tag{18}$$

where

$$K_I^{BA^i}(z', a) = (\lambda + 2\mu)\int\int_{A^i} h_{I_{y,y}}(\mathbf{r}; z', a)T(\mathbf{r})\,dA^i(\mathbf{r}). \tag{19}$$

To determine $T(\mathbf{r})$, $\mathbf{r} \in A^i$, we follow the superposition procedure described earlier and write the traction-free condition on crack A^1 or A^2, using (7) and (8). The resulting integral equation on A^1 or A^2 is

$$\int\int_{A^1}\left[8\mu^2 T(\tilde{\mathbf{r}})H(\mathbf{r}, \tilde{\mathbf{r}}) + \frac{\mu}{4\pi(1-\nu)}(R_{,x}T_{,x} + R_{,z}T_{,z})\frac{1}{R^2}\right]d\tilde{A}$$
$$+ \int\int_{A^2}[8\mu^2 T(\tilde{\mathbf{r}})H(\mathbf{r}, \tilde{\mathbf{r}}) + S^{(d)}(\mathbf{r}, \tilde{\mathbf{r}})T(\tilde{\mathbf{r}})]\,d\tilde{A} + \sigma_{yy}^{\infty}(\mathbf{r}) = 0. \tag{20}$$

The first term on the left-hand side of (20) reflects the mutual interaction of penny cracks, whereas the third and fourth terms reflect their interaction with the half-plane crack. Because of the indicated mirror symmetry about the plane $y = 0$, (20) may be written as

$$\int\int_{\tilde{x}^2+\tilde{z}^2\leqslant a^2} 8\mu^2\Big\{T(\tilde{\mathbf{r}})[H(x, y, z, \tilde{x}, \tilde{y}, \tilde{z}) + H(x, y, z, \tilde{x}, -\tilde{y}, \tilde{z})]$$
$$+ S^{(d)}(x, y, z, \tilde{x}, -\tilde{y}, \tilde{z})T(\tilde{\mathbf{r}}) + \frac{\mu}{4\pi(1-\nu)}(R_{,x}T_{,x} + R_{,z}T_{,z})\frac{1}{R^2}\Big\}d\tilde{x}\,d\tilde{z} + \sigma_{yy}^{\infty}(\mathbf{r}) = 0, \tag{21}$$

where

$$R = \sqrt{(x-\tilde{x})^2 + (z-\tilde{z})^2}, \tag{22}$$

$$S^{(d)}(x,y,z,\tilde{x},\tilde{y},\tilde{z}) = \frac{(1-2\nu)\mu}{4\pi(1-\nu)}\left[\frac{3(1+2\nu)}{(1-2\nu)}\frac{d^2}{R^5} - \frac{15}{(1-2\nu)}\frac{d^4}{R^7} + \frac{2(1-\nu)}{(1-2\nu)R^3}\right], \tag{23}$$

and $H(\mathbf{r},\tilde{\mathbf{r}})$ is given in Appendix A.

As before, define the bilinear form

$$B(T,T') = \int\int_{x^2+z^2\leqslant a^2} \mathrm{d}x\,\mathrm{d}z \int\int_{\tilde{x}^2+\tilde{z}^2\leqslant a^2} \Big\{-[8\mu^2(H(\mathbf{r},\tilde{x},\tilde{y},\tilde{z}) + H(\mathbf{r},\tilde{x},-\tilde{y},\tilde{z})$$

$$+S^{(d)}(\mathbf{r},\tilde{x},-\tilde{y},\tilde{z})]T(\tilde{\mathbf{r}})T'(\mathbf{r}) - \frac{\mu}{4\pi(1-\nu)}\left(\frac{\partial}{\partial x}\frac{1}{R}\frac{\partial T(\tilde{\mathbf{r}})}{\partial \tilde{x}} + \frac{\partial}{\partial z}\frac{1}{R}\frac{\partial T(\tilde{\mathbf{r}})}{\partial \tilde{z}}\right)T'(\mathbf{r})\Big\}\,\mathrm{d}\tilde{x}\,\mathrm{d}\tilde{z}. \tag{24}$$

Integration by parts yields:

$$B(T,T') = \int\int_{x^2+z^2\leqslant a^2} \mathrm{d}x\,\mathrm{d}z \int\int_{\tilde{x}^2+\tilde{z}^2\leqslant a^2} \Big\{-[8\mu^2(H(\mathbf{r},\tilde{x},\tilde{y},\tilde{z}) + H(\mathbf{r},\tilde{x},-\tilde{y},\tilde{z})$$

$$+S^{(d)}(\mathbf{r},\tilde{x},-\tilde{y},\tilde{z})]T(\tilde{\mathbf{r}})T'(\mathbf{r}) + \frac{\mu}{4\pi(1-\nu)}\frac{1}{R}\left(\frac{\partial T'(\mathbf{r})}{\partial x}\frac{\partial T(\tilde{\mathbf{r}})}{\partial \tilde{x}} + \frac{\partial T'(\mathbf{r})}{\partial z}\frac{\partial T(\tilde{\mathbf{r}})}{\partial \tilde{z}}\right)\Big\}\,\mathrm{d}\tilde{x}\,\mathrm{d}\tilde{z}. \tag{25}$$

Define

$$q(\mathbf{r},\tilde{\mathbf{r}}) = 8\mu^2 T(\tilde{\mathbf{r}})[H(x,y,z,\tilde{x},\tilde{y},\tilde{z}) + H(x,y,z,\tilde{x},-\tilde{y},\tilde{z})] + S^{(d)}(x,y,z,\tilde{x},-\tilde{y},\tilde{z})T(\tilde{\mathbf{r}}). \tag{26}$$

It follows then that the variational problem for the functional

$$J(T) = \tfrac{1}{2}B(T,T) - \int\int_{A^1} T(\mathbf{r})\sigma^{\infty}_{yy}(\mathbf{r})\,\mathrm{d}A(\mathbf{r}) \tag{27}$$

will lead to the unique solution of (21).

3. FINITE ELEMENT DISCRETIZATION

3.1. *Change of weak form*

In the present paper, a finite element solution will be attempted for the weak form

$$B(T,T') - (f,T') = 0 \tag{28}$$

using triangular elements, where

$$B(T,T') = \frac{\mu}{4\pi(1-\nu)}\int\int_A \mathrm{d}x\,\mathrm{d}z \int\int_A \Big\{\frac{1}{R}[T_{,\tilde{x}}(\tilde{\mathbf{r}})T'_{,x}(\mathbf{r}) + T_{,\tilde{z}}(\tilde{\mathbf{r}})T'_{,z}(\mathbf{r})] - T(\tilde{\mathbf{r}})T'(\mathbf{r})q(\mathbf{r},\tilde{\mathbf{r}})\Big\}\,\mathrm{d}\tilde{x}\,\mathrm{d}\tilde{z}, \tag{29}$$

$$(f,T') = \int\int_A f(\tilde{\mathbf{r}})T'(\tilde{\mathbf{r}})\,\mathrm{d}\tilde{x}\,\mathrm{d}\tilde{z}, \tag{30}$$

with $R = |\mathbf{r}-\tilde{\mathbf{r}}|$, and A denotes the penny-shaped crack: $\{(x,z)|(x-x_0)^2+(z-z_0)^2 \leqslant b^2\}$. It should be noted that the solution of (28) has weaker properties than the solution of the

original problem, i.e. it or its derivatives may have lesser order continuity. This is because the pointwise description of the original problem has been converted to a global integral form. Also in the weak form the kernel is less singular as the derivatives of $1/R$ have been transferred to the function $T(x, z)$. The solution of the variational problem

$$J(T_0) = \min_{T \in S^h} J(T) \tag{31}$$

with

$$J(T) = \tfrac{1}{2}B(T, T) - (f, T) \tag{32}$$

will lead to the solution of (28), where S^h refers to the linear triangular elements. As the unknown opening displacement along the edge of the crack must vanish in proportion to the square root of the distance from the edge, the opening displacement function is represented by

$$T(\mathbf{r}) = \sqrt{b^2 - c^2}\, g(\mathbf{r}), \tag{33}$$

where $c = \sqrt{(x-x_0)^2 + (z-z_0)^2}$, and $(x_0, 0, z_0)$ denotes the centre of the penny-shaped crack. The new unknown function $g(\mathbf{r})$ can be accurately approximated by the chosen linear triangular elements. Substitution of (33) into (29) yields:

$$\begin{aligned} B(T, T') = \int\int_A \mathrm{d}A \int\int_A \{ & p'(\mathbf{r}, \tilde{\mathbf{r}})[g_{,x} g'_{,\tilde{x}} + g_{,z} g'_{,\tilde{z}}] + q'(\mathbf{r}, \tilde{\mathbf{r}}) g(x, z) g'(\tilde{x}, \tilde{z}) \\ & + [(x - x_0) g'_{,\tilde{x}} + (z - z_0) g'_{,\tilde{z}}] g(x, z) s(\tilde{\mathbf{r}}, \mathbf{r}) \\ & + [(\tilde{x} - x_0) g_{,x} + (\tilde{z} - z_0) g_{,z}] g'(\tilde{x}, \tilde{z}) s(\mathbf{r}, \tilde{\mathbf{r}}) \} \, \mathrm{d}\tilde{A} \\ = B'(g, g'), & \end{aligned} \tag{34}$$

where

$$\begin{aligned} p'(\mathbf{r}, \tilde{\mathbf{r}}) &= \frac{k}{R} \sqrt{b^2 - c^2} \sqrt{b^2 - \tilde{c}^2}, \\ q'(\mathbf{r}, \tilde{\mathbf{r}}) &= \frac{k}{R} \left[\frac{(x - x_0)(\tilde{x} - x_0)}{\sqrt{b^2 - c^2}\sqrt{b^2 - \tilde{c}^2}} + \frac{(z - z_0)(\tilde{z} - z_0)}{\sqrt{b^2 - c^2}\sqrt{b^2 - \tilde{c}^2}} \right] - \sqrt{b^2 - c^2}\sqrt{b^2 - \tilde{c}^2}\, q(\mathbf{r}, \tilde{\mathbf{r}}), \\ s(\mathbf{r}, \tilde{\mathbf{r}}) &= -\frac{k}{R} \frac{\sqrt{b^2 - c^2}}{\sqrt{b^2 - \tilde{c}^2}} \end{aligned} \tag{35}$$

with $k = \mu/[4\pi(1-\nu)]$.

It is noted that the new bilinear form $B'(g, g')$ retains the positive definiteness and symmetry of $B(T, T')$. Likewise, the new kernel function retains the singularity of the old kernel function. The new weak form is

$$B'(g, g') - (f', g') = 0, \tag{36}$$

where $f' = f(\mathbf{r})\sqrt{b^2 - c^2}$, and the energy integral is

$$J'(T) = \tfrac{1}{2}B'(T, T) - (f', T). \tag{37}$$

In the sequel the prime on J' and B' will be omitted for clarity of presentation.

3.2. *Stiffness matrix and generalized load vector*

An arbitrary function g^h in the linear triangular finite element discretization can be expressed in terms of its nodal values $g_\gamma = g(x_\gamma, z_\gamma)$, $\gamma = 1,2,3$ and the shape functions $N_\gamma(x,z)$ for the element A_e

$$g^h = \sum_{\gamma=1}^{3} g_\gamma N_\gamma(x,z), \tag{38}$$

where

$$N_\gamma(x,z) = a_\gamma + b_\gamma x + c_\gamma z \tag{39}$$

is the shape function for A_e, and $A = \bigcup_{e=1}^{E} A_e$. Let the subscripts e and e' denote integration over the respective triangular element e or e', so that the energy integral (37) may be written as

$$J(g^h) = \sum_{e=1}^{E} J_e(g^h) = \sum_{e=1}^{E}\sum_{e'=1}^{E} J_{ee'}(g^h). \tag{40}$$

In terms of g^h, the energy integral $J_e(g^h)$ on the element A_e is a second order polynomial in the nodal values (g_1, g_2, g_3):

$$J_e(g^h) = \frac{1}{2}\sum_{e'=1}^{E}\sum_{\gamma=1}^{3}\sum_{\gamma'=1}^{3} g_\gamma g_{\gamma'} B_{ee'}(N_\gamma, N_{\gamma'}) - \sum_{\gamma=1}^{3}(N_\gamma, f')_e g_\gamma. \tag{41}$$

The condition for the minimum of $J_e(g^h)$ gives

$$\frac{\partial J_e}{\partial g_\gamma} = \sum_{e'=1}^{E}\sum_{\gamma'=1}^{3} g_{\gamma'} B_{ee'}(N_\gamma, N_{\gamma'}) - (N_\gamma, f')_e = 0; \quad e = 1,\ldots,E, \quad \gamma = 1,2,3. \tag{42}$$

Denote $K^{ee'}_{\gamma\gamma'} = B_{ee'}(N_\gamma, N_{\gamma'})$, and $K^{e}_{\gamma\gamma'} = \sum_{e'=1}^{E} K^{ee'}_{\gamma\gamma'}$, then $[K^e_{\gamma\gamma'}]$ is the element stiffness matrix, while $[f^e_\gamma]$ with $f^e_\gamma = (N_\gamma, f')_e$ is the element generalized load vector.

4. A SIMPLE APPROXIMATE SOLUTION

Before presenting the finite element solution of (36), we propose a simple approximate solution by assuming that the unknown opening displacement $T(\mathbf{r})$ can be replaced by $T(\mathbf{r}) = g_0\sqrt{b^2-c^2}$. It is obvious that this replacement will be the more accurate the further away the penny crack is from the half-plane crack. In the limit of this distance tending to infinity we have the exact solution, for a penny-shaped crack of radius b centred at $(x_0, 0, z_0)$ and subject to a uniform pressure p (Sneddon, 1946), for which $g_0 = p/(k\pi^2)$. In this limiting case the bilinear form $B(T,T)$ is greatly simplified and can be exactly evaluated:

$$B(T,T) = g_0^2 k \int\int_A\int\int_A \frac{\nabla\sqrt{b^2-c^2}\,\tilde{\nabla}\sqrt{b^2-\tilde{c}^2}}{R}\,\mathrm{d}A\,\mathrm{d}\tilde{A} = g_0^2\frac{2k}{3}\pi^3 b^3 = 20.6708 k b^3 g_0^2. \tag{43}$$

In the presence of the half-plane crack, the bilinear form (34), with $g(x,z) = g_0$, becomes

$$B(T,T') = kg_0^2\int\int_A\int\int_A \frac{1}{R}\left[\frac{(x-x_0)(\tilde{x}-x_0)}{\sqrt{b^2-c^2}\sqrt{b^2-\tilde{c}^2}} + \frac{(z-z_0)(\tilde{z}-z_0)}{\sqrt{b^2-c^2}\sqrt{b^2-\tilde{c}^2}}\right]\mathrm{d}A\,\mathrm{d}\tilde{A}$$

$$-g_0^2\int\int_A\int\int_A \sqrt{b^2-c^2}\sqrt{b^2-\tilde{c}^2}\,q(\mathbf{r},\tilde{\mathbf{r}})\,\mathrm{d}A\,\mathrm{d}\tilde{A}$$

$$= g_0^2\left[20.6708b^3k - \int\int_A \mathrm{d}A \int\int_A \sqrt{b^2-c^2}\sqrt{b^2-\tilde{c}^2}\, q(\mathbf{r},\tilde{\mathbf{r}})\,\mathrm{d}A\right], \tag{44}$$

where

$$q(\mathbf{r},\tilde{\mathbf{r}}) = \frac{2}{\pi}k\frac{1}{R^3}\left[\frac{R}{2\sqrt{(x-a)(\tilde{x}-a)}} - \arctan\frac{R}{2\sqrt{(x-a)(\tilde{x}-a)}}\right] \tag{45}$$

with

$$R = \sqrt{(x-\tilde{x})^2+(z-\tilde{z})^2+(y-\tilde{y})^2} = \sqrt{(x-\tilde{x})^2+(z-\tilde{z})^2}. \tag{46}$$

Similarly,

$$(f', T) = \int\int_A f(\mathbf{r})\sqrt{b^2-c^2}\, g_0\,\mathrm{d}A = g_0\int\int_A \sqrt{b^2-c^2}\, f(\mathbf{r})\,\mathrm{d}A, \tag{47}$$

where

$$f(r) = \frac{K_\mathrm{I}^\infty}{\sqrt{2\pi\rho}}, \tag{48}$$

$$\rho = \sqrt{(x-a)^2+y^2} = |x-a|. \tag{49}$$

Substituting (44) and (47) into (36) gives

$$\frac{g_0}{K_\mathrm{I}^\infty} = \frac{\displaystyle\int\int_A \sqrt{b^2-c^2}/(\sqrt{2\pi\rho})\,\mathrm{d}A}{\displaystyle 20.6708 - \int\int_A \mathrm{d}A\int\int_A \sqrt{b^2-c^2}\sqrt{b^2-\tilde{c}^2}\, q\,\mathrm{d}\tilde{A}}. \tag{50}$$

Finally, from (4) one obtains the increment in the stress intensity factor $K_\mathrm{I}^{BA}(z_1, a)$ induced along the half-plane crack front $z = z_1$ by the penny crack to be

$$\begin{aligned} K_\mathrm{I}^{BA} &= \sqrt{2/\pi}k\int\int_A \frac{T(x,0,z)}{\sqrt{\rho}[(x-a)^2+(z-z_1^2+y^2)]}\,\mathrm{d}x\,\mathrm{d}z \\ &= \sqrt{2/\pi}k\int\int_A \frac{g_0\sqrt{b^2-c^2}\,\mathrm{d}x\,\mathrm{d}z}{\sqrt{x-a}[(x-a)^2+(z-z_1)^2]}. \end{aligned} \tag{51}$$

The superposition of K_I^∞ and K_I^{BA} gives the total stress intensity factor at $z = z_1$ along the half-plane crack front. The procedure for obtaining the simple approximate solution of (36) explained above with reference to a single penny crack interacting with the half-plane crack can be generalized to many penny cracks. Several numerical examples will be given in the next section together with the finite element solution, where it will be shown that the results given by the simple approximate procedure are in excellent agreement with those of Laures and Kachanov (1991). This is not surprising in that their simplifying assumption whereby the unknown average traction over the penny crack is assumed to be uniform is equivalent to the simplifying assumption made above.

5. NUMERICAL SOLUTION AND DISCUSSION

The integration of the double integrals in the bilinear form (34) can present numerical difficulties because of the singular terms $1/R$ and $1/\sqrt{b^2-c^2}$ in the kernel. To reduce these difficulties it is customary to employ a variable finite element mesh which gets finer as the

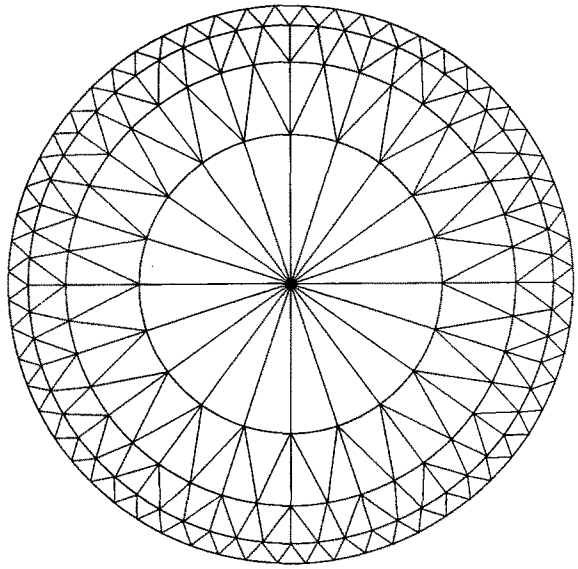

Fig. 2. Division of a circular region into 300 triangular elements of increasing fineness as the crack edge is approached.

edge of the penny-shaped crack is approached (Fig. 2). In the examples reported below, sufficient accuracy was attained by dividing each circular region into 300 triangular elements with 181 nodes. Within each triangle the double integrals were evaluated by 6 and 7 point Gaussian quadrature formulae for triangles proposed by Cowper (1972). The accuracy of the finite element solution was judged by comparing it with the known exact value of the bilinear form $B(T, T)$ for an isolated penny-shaped crack (43). The indicated subdivision of the circular region gave the value 19.5170, while the constant g_0 was found to be 0.107311 which is within 0.6% of the exact value. When the number of triangular elements was increased to 480 (with 281 nodes) the numerical value changed to 19.9643 and constant g_0 to 0.1049 which is only about 0.35% off the exact value. A similar accuracy can be expected in the general interaction case because the kernel is a product of the kernel for an isolated penny-shaped crack and a bounded linear triangular finite element basis.

5.1. *A penny-shaped crack coplanar with half-plane crack*

Let the distance separating the edge of the penny-shaped crack closest to the half-plane front be denoted in a dimensionless form by $\delta = (x_0 - a - b)/(2b)$. A typical plot of the open penny-shaped crack in mode I (for $\delta = 0.25$) is shown in Fig. 3. The contours of crack opening displacement are shown in Fig. 4. As expected, the influence of the half-plane crack on the opening displacement of the penny-shaped crack is the stronger the closer the latter is to the former. Figures 5–7 show the variation of $g(\mathbf{r})$ along the leading diagonal of the penny-shaped crack ($z = 0$) for three values of δ. It is clear that $g(\mathbf{r})$ tends to a constant value with increasing δ, lending support to the accuracy of the simple approximate solution presented in Section 4. Figure 8 shows the variation of the stress intensity factor (SIF) $K_I = K_I^\infty + K_I^{BA}$ normalized by K_I^∞. For the present geometry K_I is always greater than K_I^∞ with the maximum being attained at the point on the front that lies on the line of symmetry $z = z_0 (= 0)$. Table 1 compares the FEM result with that of Laures and Kachanov (1991). The entries in Table 1 confirm the earlier statement that the simple approximate solution (Section 4) is in excellent agreement with the solution of Laures and Kachanov (1991) and that both these solutions tend to approach the finite element solution when the penny-shaped crack is well away from the half-plane crack front.

5.2. *Two coplanar penny-shaped cracks in front of a half-plane crack*

Figure 9 shows the variation of mode I SIF along the front of the half-plane crack for various values of $\delta = (x_0 - a - b)/(2b)$ in the presence of two penny-shaped cracks lying in

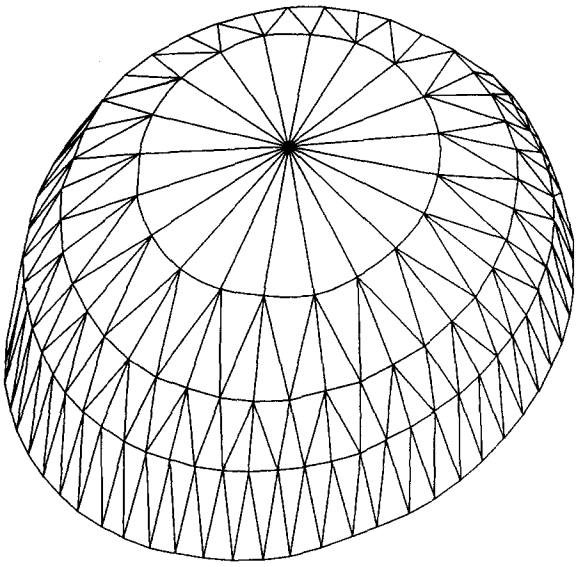

Fig. 3. A perspective of the open upper half of a penny-shaped crack in mode I for $\delta = 0.25$.

the plane $y = 0$ with centres at $(x_0, 0, z_0)$ and $(x_0, 0, -z_0)$. The distance between the centres as a proportion of their (equal) diameter is assumed to be 1.2. The maximum value of K_I is no longer attained along the line of symmetry $z = 0$ but at two points $|z_1|/b = 1.2$. Moreover, the peak value of K_I is larger than that for a single penny-shaped crack (Fig. 8). This stronger influence may be attributed to the additional interaction between the penny cracks themselves which is taken into account in the present method. The simple approximate solution can be obtained in a similar manner to that explained above with q replaced by (11) and K_I obtained by superposing K_I^∞ with $K_I^{BA^1}$ and $K_I^{BA^2}$. Table 2 gives the maximum value of K_I/K_I^∞ along the half-plane crack front and compares it with the corresponding value in the presence of just one penny-shaped crack.

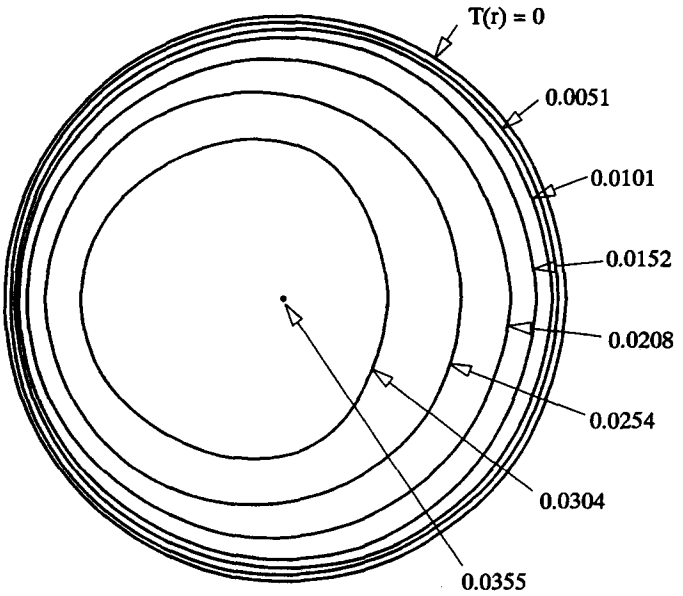

Fig. 4. Contours of the crack opening displacement corresponding to Fig. 3. Note that the contours are bunched together on the side closer to the half-plane crack.

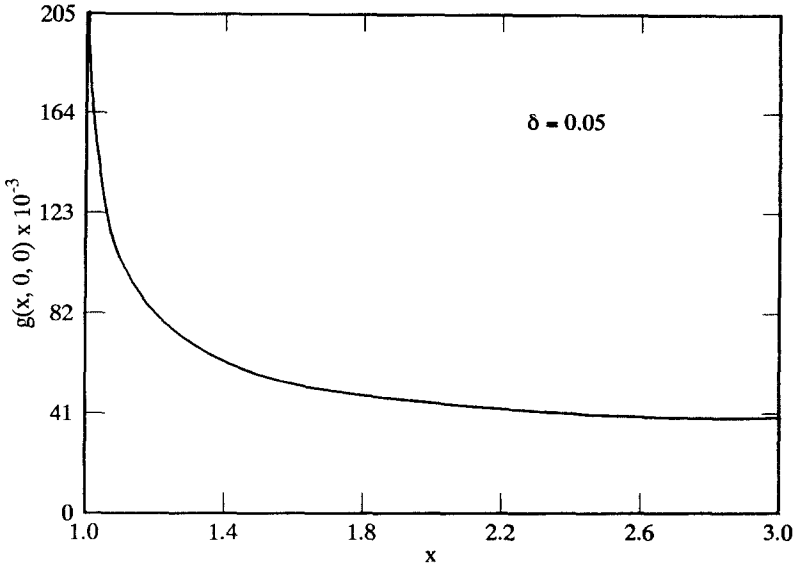

Fig. 5. Variation of $g(\mathbf{r})$ along the plane $z = 0$ for $\delta = 0.05$.

5.3. *Interaction of a half-plane crack with two off-plane parallel cracks*

Consider two symmetrically located off-plane cracks parallel to the half-plane crack under mode I loading. The vertical distance d between these two penny-shaped cracks as a fraction of their (equal) diameter is assumed to be 0.3 throughout this subsection. The choice of d must ensure that it is larger than the expected opening displacement when all the interactions are considered, so the two penny-shaped cracks will not touch each other. Denote $\delta = (x_0 - a)/b$. When a part of a penny-shaped crack is located directly above the main crack edge ($\delta < 1$), the interaction produces a strong shielding effect for K_I at points of the main crack front which are located directly under the crack. The effect changes to one of amplification beyond this region reaching the maximum value at the point under the edge of the crack and then dropping to zero as z_1 increases.

As δ increases the zone of shielding shrinks and disappears altogether at $\delta = 1$. The variation of mode I SIF along the main crack front for several different values of δ is shown

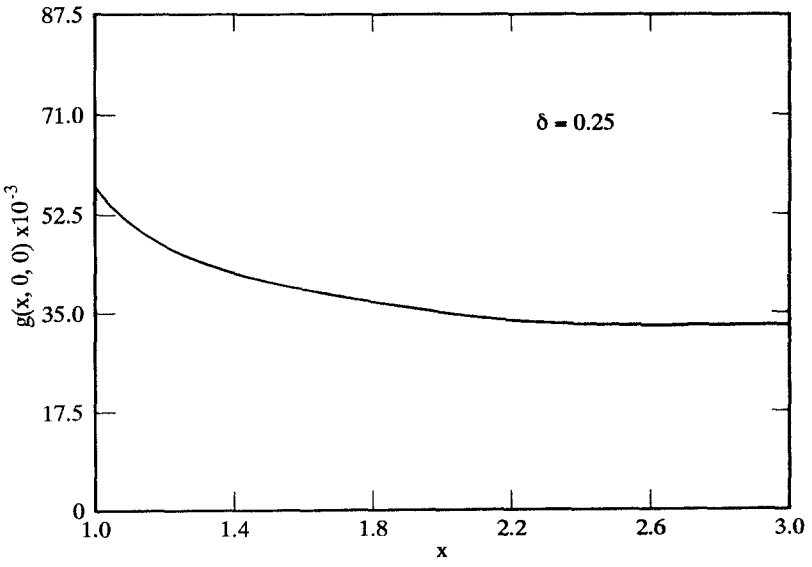

Fig. 6. Variation of $g(\mathbf{r})$ along the plane $z = 0$ for $\delta = 0.25$.

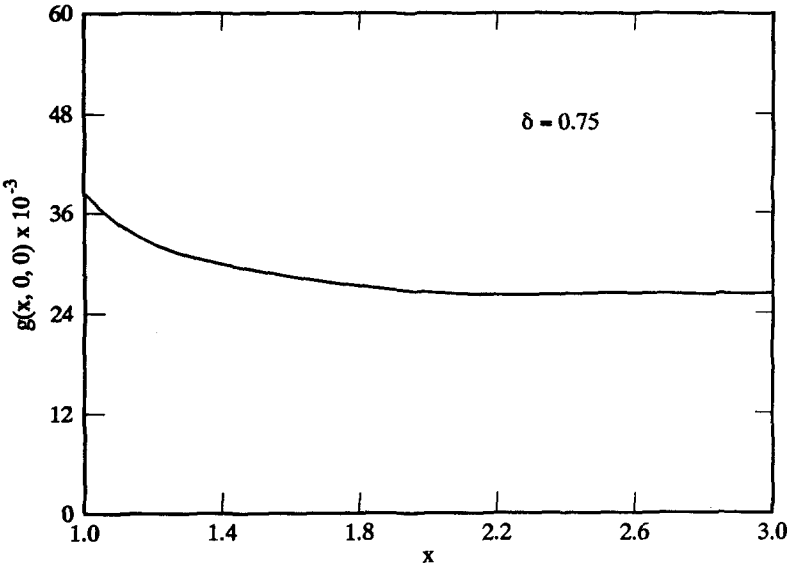

Fig. 7. Variation of $g(\mathbf{r})$ along the plane $z = 0$ for $\delta = 0.75$.

in Fig. 10. Table 3 shows the maximum and minimum values of K_I/K_I^∞ along the half-plane crack for various δ.

An approximate formula for the interaction contribution to K_I may be obtained by assuming $z = \tilde{z}$, $x = \tilde{x}$, $y = \tilde{y}$ in eqn (A23) of Appendix A, such that

$$g(\theta) = (-9 - 5.75 \sin^2\theta - 4.5 \sin^4\theta) \cos\theta, \tag{52}$$

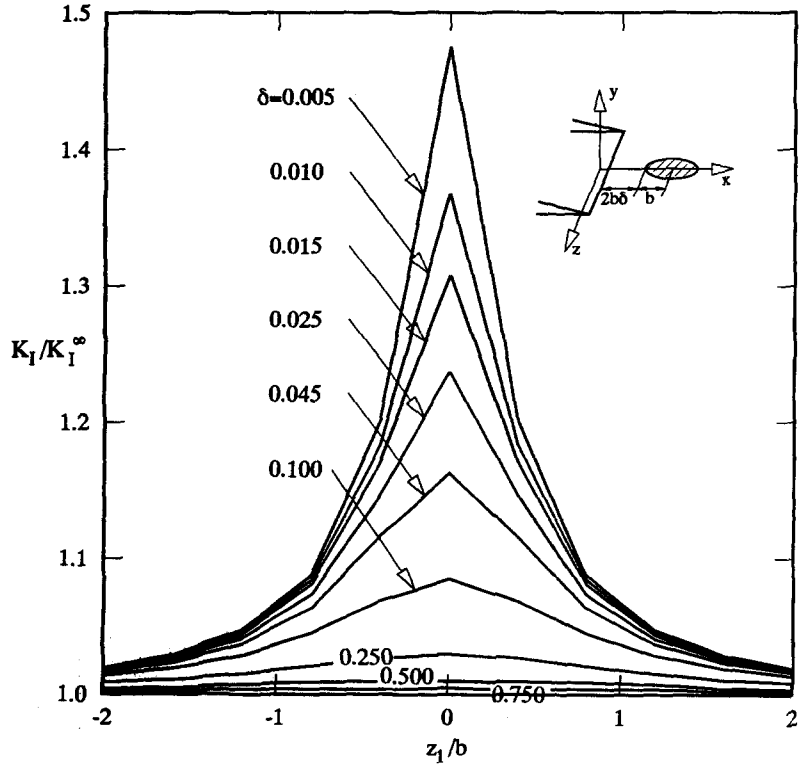

Fig. 8. Variation of K_I/K_I^∞ along the half-plane crack front in the presence of a penny-shaped crack centered at $(x_0, 0, 0)$. Note that the maximum is attained at $z = z_0\,(= 0)$.

Table 1. Maximum values of K_I/K_I^∞ at $z_1 = z_0$ along the front of a half-plane crack due to interaction with a coplanar penny-shaped crack centered at $(x_0, 0, 0)$

δ	Laures and Kachanov (1991)	Approximate method eqn (51)	F.E.M.
0.005	1.48	1.476	1.9807
0.010	1.37	1.368	1.8172
0.015	1.31	1.308	1.6310
0.025	1.24	1.237	1.4374
0.045	1.17	1.165	1.2701
0.100	1.09	1.086	1.1228
0.250	1.03	1.030	1.0383
0.500	1.01	1.010	1.0124
0.750	1.005	1.005	1.0057

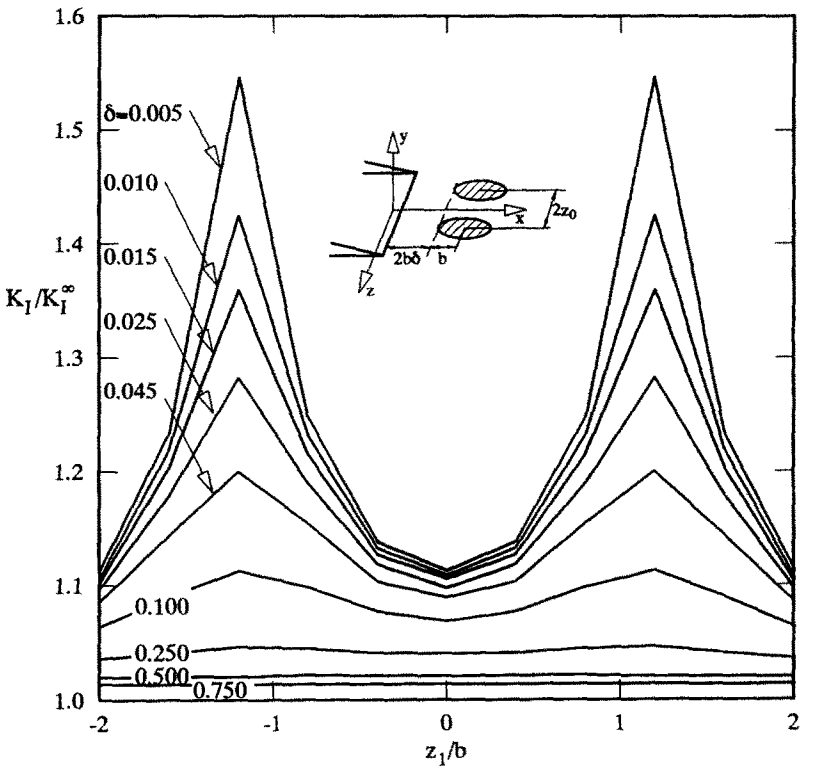

Fig. 9. Variation of K_I/K_I^∞ along the half-plane crack front in the presence of two identical penny-shaped cracks centered at $(x_0, 0, z_0)$ and $(x_0, 0, -z_0)$, with $|z_0|/b = 1.2$. Note that the two (equal) peak values are larger than that in the presence of a single penny-shaped crack (Fig. 8).

Table 2. Maximum K_I/K_I^∞ at $|z_1| = |z_0|$ along the half-plane crack front in the presence of two coplanar penny-shaped cracks

δ	Two coplanar penny cracks	One coplanar penny crack
0.005	1.5446	1.476
0.010	1.4242	1.368
0.015	1.3565	1.308
0.025	1.2770	1.237
0.045	1.1954	1.165
0.100	1.1063	1.086
0.250	1.0408	1.030

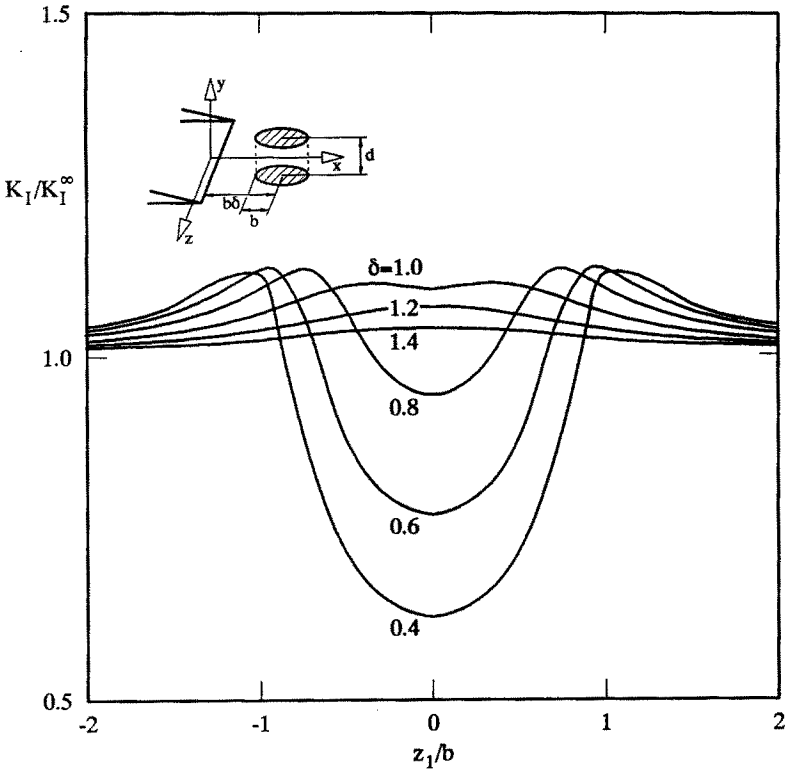

Fig. 10. Variation of K_I/K_I^∞ along the half-plane crack front in the presence of two off-plane parallel penny-shaped cracks for different values of $\delta = (x_0-a)/b$ and $d/b = 0.3$.

$$f(\theta) = 0.3+1.55\sin^2\theta+\sin^4\theta-14\sin^6\theta, \tag{53}$$

$$I_4 = \frac{-(x_0-a)}{2y_0^2\rho_0^2}+\frac{1}{2y_0^3}\left(\frac{\pi}{2}-\arctan\frac{x_0-a}{y_0}\right), \tag{54}$$

where

$$8\mu^2 H = \frac{k}{8\pi}\left\{\frac{1}{\rho_0^3}[g(\theta)+f(\theta)]+28I_4\right\}, \tag{55}$$

$$\rho_0 = \sqrt{(x_0-a)^2+y_0^2}, \quad \cos\theta = \frac{x_0-a}{\rho_0}, \quad \sin\theta = \frac{y_0}{\rho_0}. \tag{56}$$

Finally, (4) may be written as:

Table 3. K_I/K_I^∞ along the half-plane crack under mode I loading in the presence of two symmetrically located parallel penny-shaped cracks

δ	Max.	Min.
0.4	1.1268	0.6177
0.6	1.1310	0.7685
0.8	1.1238	0.9416
1.0	1.0985	1.0000
1.2	1.0702	1.0000
1.4	1.0385	1.0000

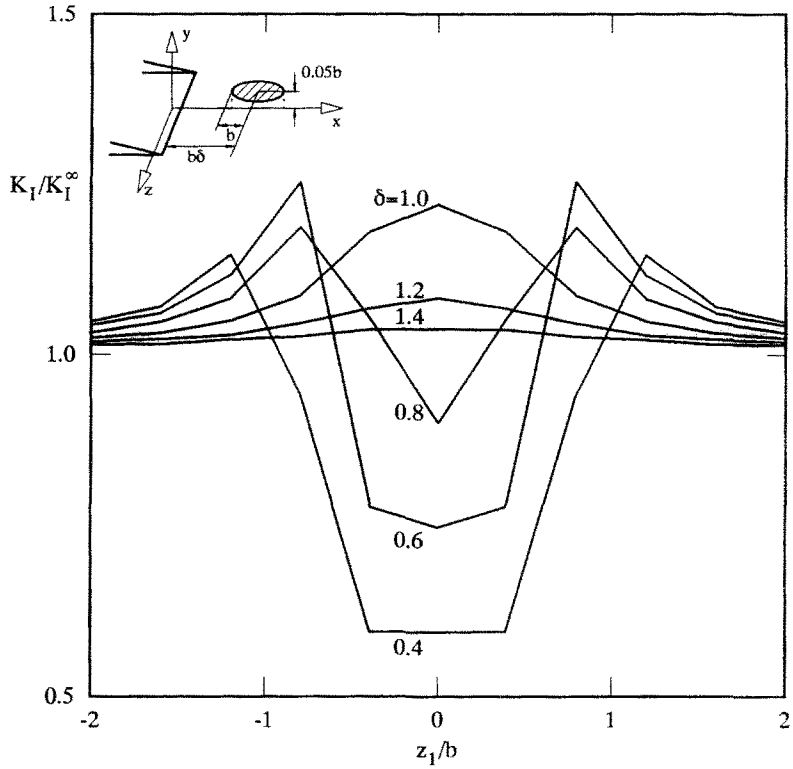

Fig. 11. Variation of K_I/K_I^∞ along the half-plane crack front in the presence of a single penny-shaped crack slightly off the plane of symmetry ($y_0 = 0.05b$) for different values of $\delta = (x_0-a)/b$.

$$K_I^{BA'}(z',a) = \sqrt{\frac{2}{\pi}}\, k \iint_{A'} \frac{\cos(\phi/2)[(1-8\rho^2/R^2\sin^2\phi/2)]}{R^2\sqrt{\rho}}\, T'(\mathbf{r})\, \mathrm{d}A'(\mathbf{r}). \tag{57}$$

5.4. *Interaction of a half-plane crack with one off-plane penny-shaped crack*

The model in this paper can only deal with mode I loading. But when the vertical distance of one off-plane crack from the half-plane crack is very small, the shear effects may be neglected. By using the approximate formula, the mode I SIF along the main crack front for several different values of $\delta = (x_0-a)/b$ and vertical distance $y_0 = 0.05b$ was calculated and the results are shown in Fig. 11. The maximum and minimum values are listed in Table 4 and compared with those of Laures and Kachanov (1991). When a part of the crack is above the half-plane crack edge ($\delta < 1$) the interaction produces a shielding effect for K_I at the point of the half-plane crack edge located directly under the crack; the effect changes to the one of amplification beyond this region and vanishes quickly at points further along the edge. As δ increases, the zone of shielding shrinks and disappears altogether at $\delta = 1$.

Table 4. K_I/K_I^∞ along the half-plane crack under mode I loading in the presence of a single off-plane parallel penny-shaped crack

δ	Max. (Laures and Kachanov)	Max.	Min. (Laures and Kachanov)	Min.
0.4	1.372	1.253	0.596	0.593
0.6	1.419	1.252	0.699	0.714
0.8	1.442	1.269	0.879	0.898
1.0	1.379	1.225	1.000	1.000
1.2	1.091	1.083	1.000	1.000
1.4	1.042	1.040	1.000	1.000

REFERENCES

Bueckner, H. F. (1987). Weight functions and fundamental fields for the penny-shaped and the half-plane crack in three-space. *Int. J. Solids Structures* **23,** 57–93.

Bui, H. D. (1977). An integral equations method for solving the problem of a plane crack of arbitrary shape. *J. Mech. Phys. Solids* **25,** 29–39.

Cowper, G. R. (1972). Gaussian quadrature formulas for triangles. *Int. J. Numer. Meth. Engng* **7,** 405–408.

Cruse, T. A. (1969). Numerical solutions in three dimensional elastostatics. *Int. J. Solids Structures* **5,** 1259–1274.

Gong, S. X. and Horii, H. (1989). General solution to the problem of microcracks near the tip of a main crack. *J. Mech. Phys. Solids* **37,** 27–46.

Horii, H. and Nemat-Nasser, S. (1985). Elastic fields of interacting inhomogeneities. *Int. J. Solids Structures* **21,** 731–745.

Huang, X. and Karihaloo, B. L. (1992). Tension softening of quasi-brittle materials modelled by singly and doubly periodic arrays of coplanar penny-shaped cracks. *Mech. Mater.* **13,** 257–275.

Karihaloo, B. L. and Huang, X. (1989). Three-dimensional elastic crack tip interactions with shear transformation strains. *Int. J. Solids Structures* **25,** 591–607.

Kupradze, V. D. (1963). *Dynamical Problems in Elasticity*. North-Holland, Amsterdam.

Laures, J. P. and Kachanov, M. (1991). Three-dimensional interactions of a crack front with arrays of penny-shaped microcracks. *Int. J. Fract.* **48,** 255–279.

Rice, J. R. (1985). Three-dimensional elastic crack tip interactions with transformation strains and dislocations. *Int. J. Solids Structures* **21,** 781–791.

Rose, L. R. F. (1986). Microcrack interaction with a main crack. *Int. J. Fract.* **31,** 233–242.

Rubinstein, A. A. (1986). Macrocrack–microdefect interaction. *J. Appl. Mech.* **53,** 781–791.

Shum, D. K. M. and Hutchinson, J. W. (1990). On toughening by microcracks. *Mech. Mater.* **9,** 83–91.

Sneddon, I. N. (1946). The distribution of stress in the neighbourhood of a crack in an elastic solid. *Proc. R. Soc. London* **A187,** 229–260.

Note added in proof

In Section 2.2 the contributions of T_x and T_z to K_I were not included. Further work is required to quantify precisely these contributions. The "curves" shown on Figs 8, 9 and 11 are only intended to link up specific points for which detailed computations were carried out. These points should have been joined by smooth curves showing a smooth maximum, as in Fig. 10.

APPENDIX A. CALCULATION OF $H(\mathbf{r},\tilde{\mathbf{r}})$ IN MODE I

In mode I

$$H(\mathbf{r},\tilde{\mathbf{r}}) = \int_{-\infty}^{-\infty}\int_{-\infty}^{a} [P_{,y} - yP_{,yy}][\tilde{P}_{,\tilde{y}} - \tilde{y}\tilde{P}_{,\tilde{y}\tilde{y}}]\,\mathrm{d}z'\,\mathrm{d}a, \tag{A1}$$

where

$$P_{,y} = -\frac{C_0\sqrt{2\rho}\cos\dfrac{\phi}{2}}{2\rho R'^2}\left[1-4\frac{\rho^2}{R'^2}(1-\cos\phi)\right], \tag{A2}$$

$$P_{,yy} = \frac{C_0\sqrt{2\rho}\sin\dfrac{\phi}{2}}{4\rho^2 R'^2}\left[(1+2\cos\phi)+8\frac{\rho^2}{R'^2}(2+\cos\phi)-32\frac{\rho^2}{R'^4}y^2\right], \tag{A3}$$

with

$$R' = \sqrt{(x-a)^2+y^2+(z-z')^2},$$
$$\rho = \sqrt{(x-a)^2+y^2}, \tag{A4}$$

$$C_0 = -\frac{1}{4(1-\nu)\pi^{3/2}}. \tag{A5}$$

Denote

$$F_{mn}(\tilde{\mathbf{r}},\mathbf{r},a) = \int_{-\infty}^{+\infty}\frac{\mathrm{d}z'}{[(\tilde{x}-a)^2+\tilde{y}^2+(\tilde{z}-z')^2]^m[(x-a)^2+y^2+(z-z')^2]^n}, \tag{A6}$$

which will be calculated in Appendix B. Substituting F_{mn} and $P_{,y}$, $P_{,yy}$ into (A1) yields,

$$H = \int_{-\infty}^{a}\left\{\frac{C_0^2}{2}\frac{\cos(\phi/2)\cos(\tilde{\phi}/2)}{\sqrt{\rho\tilde{\rho}}}f_1 + \frac{yC_0^2}{4}\frac{\sin(\phi/2)\cos(\tilde{\phi}/2)}{\sqrt{\rho\tilde{\rho}\rho}}f_2 + \frac{\tilde{y}C_0^2}{4}\frac{\sin(\tilde{\phi}/2)\cos(\phi/2)}{\sqrt{\rho\tilde{\rho}\tilde{\rho}}}f_3 + \frac{y\tilde{y}C_0^2}{8}\frac{\sin(\phi/2)\sin(\tilde{\phi}/2)}{\sqrt{\rho\tilde{\rho}\rho\tilde{\rho}}}f_4\right\}\mathrm{d}a, \tag{A7}$$

where

$$f_1 = F_{11} - 4\rho^2(1-\cos\phi)F_{12} - 4\tilde{\rho}^2(1-\cos\tilde{\phi})F_{21} + 16\rho^2\tilde{\rho}^2(1-\cos\phi)(1-\cos\tilde{\phi})F_{22},$$
$$f_2 = (1+2\cos\phi)F_{11} + 8\rho^2(2+\cos\phi)F_{12} - 4\tilde{\rho}^2(1-\cos\tilde{\phi})(1+2\cos\phi)F_{21}$$
$$-32\rho^2y^2F_{13} - 32\rho^2\tilde{\rho}^2(1-\cos\tilde{\phi})(2+\cos\phi)F_{22} + 128\rho^2\tilde{\rho}^2y^2(1-\cos\tilde{\phi})F_{23},$$

$$f_3 = (1+2\cos\tilde{\phi})F_{11}+8\tilde{\rho}^2(2+\cos\tilde{\phi})F_{21}-4\rho^2(1-\cos\phi)(1+2\cos\tilde{\phi})F_{12}$$
$$-32\tilde{\rho}^2\tilde{y}^2F_{31}-32\rho^2\tilde{\rho}^2(1-\cos\phi)(2+\cos\phi)F_{22}+128\rho^2\tilde{\rho}^2\tilde{y}^2(1-\cos\phi)F_{32},$$
$$f_4 = (1+2\cos\phi)(1+2\cos\tilde{\phi})F_{11}+64\rho^2\tilde{\rho}^2(2+\cos\phi)(2+\cos\phi)F_{22}$$
$$+1024\rho^2\tilde{\rho}^2y^2\tilde{y}^2F_{33}+8\rho^2(2+\cos\phi)(1+2\cos\tilde{\phi})F_{12}+8\tilde{\rho}^2(2+\cos\tilde{\phi})(1+2\cos\phi)F_{21}$$
$$-32\rho^2y^2(1+2\cos\tilde{\phi})F_{13}-32\tilde{\rho}^2\tilde{y}^2(1+2\cos\phi)F_{31}$$
$$-256\rho^2\tilde{\rho}^2\tilde{y}^2(2+\cos\phi)F_{32}-256\rho^2\tilde{\rho}^2y^2(2+\cos\tilde{\phi})F_{23}. \tag{A8}$$

For brevity $F_{mn}(\tilde{\mathbf{r}},\mathbf{r},a)$ have been simply written as F_{mn} in (A7). Further analytic manipulation is difficult without additional assumptions. But numerical solution is made easier when the range of integration $(-\infty,a)$ is transferred to a finite segment $(0,\phi_0)$ where

$$\phi_0 = \arctan\frac{y_0}{x_0-a}. \tag{A9}$$

In the most general case, the following relation between ϕ and $\tilde{\phi}$ is true

$$\cot\tilde{\phi} = \frac{\tilde{x}-a}{\tilde{y}} = \frac{\tilde{x}-x}{\tilde{y}}+\frac{x-a}{\tilde{y}} = \frac{\tilde{x}-a}{\tilde{y}}+\frac{y}{\tilde{y}}\cot\phi. \tag{A10}$$

Hence

$$\cos^2\tilde{\phi} = \cot^2\tilde{\phi}\sin^2\tilde{\phi}(1-\cos^2\tilde{\phi}), \tag{A11}$$

$$\cos\tilde{\phi} = \frac{\cot\tilde{\phi}}{\sqrt{1+\cot^2\tilde{\phi}}} = \frac{\dfrac{\tilde{x}-x}{\tilde{y}}+\dfrac{y}{\tilde{y}}\cot\phi}{\sqrt{1+\left(\dfrac{\tilde{x}-x}{\tilde{y}}+\dfrac{y}{\tilde{y}}\cot\phi\right)^2}} = \frac{(\tilde{x}-x)+y\cot\phi}{\sqrt{\tilde{y}^2+(\tilde{x}-x+y\cot\phi)^2}}, \tag{A12}$$

so that

$$\cos\tilde{\phi} = \frac{(\tilde{x}-x)\tan\phi+y}{\sqrt{\tilde{y}^2\tan^2\phi+[(\tilde{x}-x)\tan\phi+y]^2}}, \tag{A13}$$

$$\sin\tilde{\phi} = \frac{\tilde{y}\tan\phi}{\sqrt{\tilde{y}^2\tan^2\phi+[(\tilde{x}-x)\tan\phi+y]^2}}, \tag{A14}$$

and from

$$\phi = \arctan\frac{y}{x-a} \tag{A15}$$

we have

$$\mathrm{d}\phi = \frac{\dfrac{y}{(x-a)^2}\mathrm{d}a}{1+\left(\dfrac{y}{x-a}\right)^2} = \frac{y\,\mathrm{d}a}{(x-a)^2+y^2} = \frac{y}{\rho^2}\mathrm{d}a. \tag{A16}$$

Other useful formulae are:

$$\rho = \frac{y}{\sin\phi}, \tag{A17}$$

$$\tilde{\rho} = \frac{\tilde{y}}{\sin\tilde{\phi}} = \tilde{y}\frac{\sqrt{\tilde{y}^2\tan^2\phi+[(\tilde{x}-x)\tan\phi+y]^2}}{\tilde{y}\tan\phi} = \sqrt{\tilde{y}^2+[(\tilde{x}-x)+y\cot\phi]^2}. \tag{A18}$$

Special case 1: $x=\tilde{x}$, $y=\tilde{y}$

In this case, the penny crack A is narrow and parallel to the half-plane crack front $x=a$:

$$A = \{(x,y,z)|y=y_0, z_0\leqslant z\leqslant z_1, x_0\leqslant x\leqslant x_0+\Delta x\}. \tag{A19}$$

One may therefore assume

$$\phi = \tilde{\phi}$$

and

$$\rho = \tilde{\rho},$$

so that (A7) takes the simpler form

$$H = C_0^2 \int_{-\infty}^{a} \left\{ F_{11}\left[\frac{(1+\cos\phi)}{4\rho} + \frac{y^2}{16\rho^3}(5+7\cos\phi) + \frac{y^4}{4\rho^5}\cos\phi\right] + F_{22}\frac{4y^4}{\rho}(1+\cos\phi) \right.$$
$$+ F_{33}64y^6\rho(1-\cos\phi) + (F_{12}+F_{21})\left[\frac{y^2}{\rho}(1+\cos\phi) + \frac{y^4}{2\rho^3}(1+2\cos\phi)\right]$$
$$\left. + (F_{13}+F_{31})\left[-\frac{2y^4}{\rho}(1+\cos\phi) - \frac{4y^6}{\rho^3}\right] - (F_{32}+F_{23})\frac{16y^6}{\rho}\right\} da. \quad \text{(A20)}$$

F_{mn} are also simplified:

$$F_{11} = \frac{2\pi}{\rho}F,$$
$$F_{22} = \frac{\pi}{2}\left[\frac{10}{\rho^3}F^2 - \frac{8(z-\tilde{z})^2}{\rho^3}F^3\right],$$
$$F_{33} = \frac{3\pi}{8}\left[\frac{42}{\rho^5}F^3 - \frac{40(z-\tilde{z})^2}{\rho^5}F^4 - \frac{128(z-\tilde{z})^2}{\rho^3}F^5\right],$$
$$F_{12} = F_{21} = \frac{\pi}{\rho^3}[\tfrac{1}{2}F - (z-\tilde{z})^2F^2],$$
$$F_{31} = F_{13} = \frac{\pi}{8}\left[\frac{3}{\rho^5}F + \frac{28}{\rho^3}F^2 - \frac{16(z-\tilde{z})^2}{\rho^3}F^3\right],$$
$$F_{32} = F_{23} = \frac{\pi}{8}\left[\frac{35}{\rho^5}F^2 - \frac{32(z-\tilde{z})^2}{\rho^5}F^3 - 96\frac{(z-\tilde{z})^2}{\rho^3}F^4\right]. \quad \text{(A21)}$$

H can be expressed in powers of $F = [(z-\tilde{z})^2+(\rho+\tilde{\rho})^2]^{-1}$

$$H(\tilde{\mathbf{r}},\mathbf{r}) = C_0^2\pi \int_{-\infty}^{a} \left\{F\left[\frac{1+\cos\phi}{2\rho^2} + \frac{29+31\cos\phi}{8\rho^4}y^2 + \frac{4\cos\phi}{2\rho^6}y^4 - \frac{3y^6}{\rho^8}\right]\right.$$
$$+ F^2\left[\frac{6(1+\cos\phi)}{\rho^4}y^4 - \frac{168}{\rho^6}y^6 + (z-\tilde{z})^2\left(-\frac{2(1+\cos\phi)}{\rho^4}y^2 - \frac{1+2\cos\phi}{\rho^6}y^4\right)\right]$$
$$+ F^3\left[\frac{1008(1-\cos\phi)}{\rho^4}y^6 + (z-\tilde{z})^2\left(-\frac{8(1+\cos\phi)}{\rho^4}y^4 + \frac{144}{\rho^6}y^6\right)\right]$$
$$\left. + F^4(z-\tilde{z})^2 192\frac{(-3+5\cos\phi)}{\rho^4}y^6 + F^5(z-\tilde{z})^2\left[-\frac{3072}{\rho^2}(1-\cos\phi)y^6\right]\right\} da.$$

By use of the identity

$$(z-\tilde{z})^2F^2 = F - 4\rho^2F^2, \quad \text{(A22)}$$

we have

$$H = C_0^2\pi \int_{-\infty}^{a} \left\{F\left[\frac{1+\cos\phi}{2\rho^2} + \frac{13+15\cos\phi}{8\rho^4}y^2 - \frac{y^4}{\rho^6} - \frac{3}{\rho^8}y^6\right]\right.$$
$$+ F^2\left[\frac{8(1+\cos\phi)}{\rho^2}y^2 + \frac{2(1+3\cos\phi)}{\rho^4}y^4 - \frac{24}{\rho^6}y^6\right] + F^4\left[\frac{-768(1+\cos\phi)}{\rho^2}y^6\right]$$
$$\left. + F^3\left[\frac{32(1+\cos\phi)}{\rho^2}y^4 - \frac{48(3+\cos\phi)}{\rho^4}y^6\right] + F^5[12288(1-\cos\phi)y^6]\right\} da.$$

When $z = \tilde{z}$,

$$H = C_0^2\pi \int_{-\infty}^{a} \left[\frac{(1+\cos\phi)}{8\rho^4} + \frac{y^2}{32\rho^6}(29+31\cos\phi) + \frac{y^4}{8\rho^8}(3+7\cos\phi) + \frac{y^6}{4\rho^{10}}(18-63\cos\phi)\right] da. \quad \text{(A23)}$$

When $z \neq \tilde{z}$, we use the relation

$$\frac{F}{\rho^2} = \frac{1}{Z^2}\left(\frac{1}{4\rho^2} - F\right), \quad \text{(A24)}$$

where

$$Z^2 = \left(\frac{z-\hat{z}}{2}\right)^2, \tag{A25}$$

and express all terms of the type F^m/ρ^{2n} through $1/\rho^{2k}$ and F^k as follows:

$$\frac{F}{\rho^2} = \frac{1}{Z^2}\left[\frac{1}{4\rho^2} - F\right],$$

$$\frac{F}{\rho^4} = \frac{1}{Z^2}\left[\frac{1}{4\rho^4} - \frac{1}{4Z^2\rho^2} + \frac{F}{Z^2}\right],$$

$$\frac{F}{\rho^6} = \frac{1}{Z^2}\left[\frac{1}{4\rho^6} - \frac{1}{4Z^2\rho^4} + \frac{1}{4Z^4\rho^2} - \frac{F}{Z^4}\right],$$

$$\frac{F}{\rho^8} = \frac{1}{Z^2}\left[\frac{1}{4\rho^8} - \frac{1}{4Z^2\rho^6} + \frac{1}{4Z^4\rho^4} - \frac{1}{4Z^6\rho^2} - \frac{F}{Z^6}\right],$$

$$\frac{F^2}{\rho^2} = \frac{1}{Z^2}\left[\frac{1}{4^2Z^2\rho^2} - \frac{F}{4Z^2} - F^2\right],$$

$$\frac{F^2}{\rho^4} = \frac{1}{Z^4}\left[\frac{1}{4^2\rho^4} - \frac{2}{4^2Z^2\rho^2} + \frac{2F}{4Z^2} + F^2\right],$$

$$\frac{F^2}{\rho^6} = \frac{1}{Z^4}\left[\frac{1}{4^2\rho^6} - \frac{2}{4^2Z^2\rho^4} + \frac{3}{4^2Z^4\rho^2} - \frac{3F}{4Z^4} - \frac{F^2}{Z^2}\right],$$

$$\frac{F^3}{\rho^2} = \frac{1}{Z^2}\left[\frac{1}{4^3Z^4\rho^2} - \frac{F}{4^2Z^4} - \frac{F^2}{4Z^2} - F^3\right],$$

$$\frac{F^3}{\rho^4} = \frac{1}{Z^4}\left[\frac{1}{4^3Z^2\rho^4} - \frac{3}{4^3Z^4\rho^2} + \frac{3F}{4^2Z^4} + \frac{2F^2}{4Z^2} + F^3\right],$$

$$\frac{F^4}{\rho^2} = \frac{1}{Z^2}\left[\frac{1}{4^4Z^6\rho^2} - \frac{F}{4^3Z^6} - \frac{F^2}{4^2Z^4} - \frac{F^3}{4Z^2} - F^4\right].$$

Substituting the above expansions for F^m/ρ^{2n} into the expression for H gives:

$$\begin{aligned}
H(\mathbf{r},\tilde{\mathbf{r}}) = C_0^2\pi\int_{-\infty}^{a}\Bigg\{&\frac{(1+\cos\phi)}{2Z^2}\left[\frac{1}{4\rho^2} - F\right] + \frac{(13+15\cos\phi)}{8Z^2}y^2\left[\frac{1}{4\rho^4} - \frac{1}{4Z^2\rho^2} + \frac{F}{Z^2}\right]\\
&- \frac{y^4}{Z^2}\left[\frac{1}{4\rho^6} - \frac{1}{4Z^2\rho^4} + \frac{1}{4Z^4\rho^2} - \frac{F}{Z^4}\right] - \frac{3y^6}{Z^2}\left[\frac{1}{4\rho^8} - \frac{1}{4Z^2\rho^6} + \frac{1}{4Z^4\rho^4} - \frac{1}{4Z^6\rho^2} + \frac{F}{Z^6}\right]\\
&+ \frac{8(1+\cos\phi)y^2}{Z^2}\left[\frac{1}{4^2Z^2\rho^2} - \frac{F}{4Z^2} - F^2\right] - \frac{2(1+3\cos\phi)y^4}{Z^4}\left[\frac{1}{4^2\rho^4} - \frac{2}{4^2Z^2\rho^2} + \frac{2F}{4Z^2} + F^2\right]\\
&- \frac{24y^6}{Z^4}\left[\frac{1}{4^2\rho^6} - \frac{2}{4^2Z^2\rho^4} + \frac{3}{4^2Z^4\rho^2} - \frac{3F}{4Z^4} - \frac{F^2}{Z^2}\right]\\
&+ \frac{32(1+\cos\phi)y^4}{Z^2}\left[\frac{1}{4^3Z^4\rho^2} - \frac{F}{4^2Z^4} - \frac{F^2}{4Z^2} - F^3\right]\\
&- \frac{48(3+\cos\phi)y^6}{Z^4}\left[\frac{1}{4^3Z^2\rho^4} - \frac{3}{4^3Z^4\rho^2} + \frac{3F}{4^2Z^4} + \frac{2F^2}{4Z^2} + F^3\right]\\
&- \frac{768(1+\cos\phi)y^6}{Z^2}\left[\frac{1}{4^4Z^6\rho^2} - \frac{F}{4^3Z^6} - \frac{F^2}{4^2Z^4} - \frac{F^3}{4Z^2} - F^4\right]\\
&+ 12288(1-\cos\phi)y^6[F^5]\Bigg\}\,da.
\end{aligned} \tag{A26}$$

Collecting terms with like powers of $1/\rho^{2m}$ and F^n gives:

$$\begin{aligned}
H = C_0^2\pi\int_{-\infty}^{a}\Bigg\{&F\left[-\frac{1}{2Z^2}(1+\cos\phi) - \frac{y^2}{8Z^4}(3+\cos\phi) + \frac{y^4}{Z^6}(4+5\cos\phi) + \frac{y^6}{Z^8}(3\cos\phi)\right]\\
&+F^2\left[-8\frac{y^2}{Z^2}(1+\cos\phi) + \frac{y^4}{Z^4}(-6-2\cos\phi) + \frac{y^6}{Z^6}(24\cos\phi)\right]\\
&+F^3\left[-\frac{y^4}{Z^2}32(1+\cos\phi) + 48\frac{y^6}{Z^4}(1+3\cos\phi)\right]
\end{aligned}$$

$$+F^4\left[\frac{y^6}{768Z^2}(1+\cos\phi)\right]+F^5[12288y^6(1-\cos\phi)]$$
$$+\frac{1}{\rho^2}\left[\frac{1}{8Z^2}(1+\cos\phi)+\frac{y^2}{32Z^4}(3+\cos\phi)-\frac{y^4}{4Z^6}(\cos\phi)-\frac{y^6}{4Z^8}(3\cos\phi)\right]$$
$$+\frac{1}{\rho^4}\left[\frac{y^2}{32Z^2}(13+15\cos\phi)+\frac{y^4}{8Z^4}3(1+\cos\phi)-\frac{y^6}{4Z^6}(3\cos\phi)\right]$$
$$+\frac{1}{\rho^6}\left[-\frac{y^4}{4Z^2}-\frac{3y^6}{4Z^4}\right]+\frac{1}{\rho^8}\left[-\frac{3y^6}{4Z^2}\right]\Bigg\}\,da, \tag{A27}$$

which may then be rewritten in the following final form:

$$H=C_0^2\pi\Bigg\{\tfrac{1}{4}J_1(x-a,y^2+Z^2)\left[-\frac{1}{2Z^2}-\frac{3y^2}{8z^4}+\frac{4y^4}{Z^6}\right]$$
$$+\tfrac{1}{4}J_1(\rho_0,Z^2)\left[-\frac{1}{2Z^2}-\frac{y^2}{8Z^4}+\frac{5y^4}{Z^6}+\frac{3y^6}{Z^8}\right]$$
$$+\tfrac{1}{16}J_2(x-a,y^2+Z^2)\left[-\frac{8y^2}{Z^2}-\frac{6y^4}{z^4}\right]$$
$$+\tfrac{1}{16}J_2(\rho_0,Z^2)\left[-\frac{8y^2}{Z^2}-\frac{2y^4}{Z^4}+\frac{24y^6}{Z^6}\right]$$
$$+J_3(x-a,y^2+Z^2)\left[-\frac{y^4}{2Z^2}+\frac{3y^6}{4z^4}\right]$$
$$+J_3(\rho_0,Z^2)\left[-\frac{y^4}{2Z^2}+\frac{3y^6}{4Z^4}\right]+J_4(x-a,y^2+Z^2)\left[\frac{3y^6}{z^2}\right]$$
$$+J_4(\rho_0,Z^2)\left[3\frac{y^6}{Z^2}\right]+J_5(x-a,y^2+Z^2)[12y^6]-J_5(\rho_0,Z^2)[12y^6]$$
$$+J_1(x-a,y^2)\left[\frac{1}{8Z^2}+\frac{3y^2}{32Z^4}\right]+J_1(\rho_0,0)\left[\frac{1}{8Z^2}+\frac{y^2}{32Z^4}-\frac{y^4}{4Z^6}-\frac{3y^6}{4Z^8}\right]$$
$$+J_2(x-a,y^2)\left[\frac{13y^2}{32Z^2}+\frac{3y^4}{8Z^4}\right]+J_2(\rho_0,0)\left[\frac{15y^2}{32Z^2}+\frac{3y^4}{8Z^4}-\frac{3y^6}{4Z^6}\right]$$
$$+J_3(x-a,y^2)\left[-\frac{y^4}{4Z^2}-\frac{3y^6}{4Z^4}\right]+J_4(x-a,y^2)\left[-\frac{3y^6}{4Z^2}\right]\Bigg\}, \tag{A28}$$

where $J_n(x_0,c^2)$ stands for the recursive integral:

$$J_n(x_0,\eta^2)=\int_{x_0}^{\infty}\frac{dx}{(x^2+\eta^2)^n}=-\frac{1}{2\eta^2(n-1)(x_0^2+\eta^2)^{n-1}}+\frac{2n-3}{2\eta^2(n-1)}J_{n-1}(x_0,\eta^2), \tag{A29}$$

with

$$J_1(x_0,\eta^2)=\frac{1}{|\eta|}\left(\frac{\pi}{2}-\arctan\frac{x_0}{|\eta|}\right). \tag{A30}$$

When $\eta=0$

$$J_n(x_0,0)=\int_{x_0}^{\infty}\frac{dx}{x^{2n}}=\frac{1}{(2n-1)x_0^{2n-1}}. \tag{A31}$$

The integrals with $\cos\phi$ have been calculated using the following relation:

$$\int_{-\infty}^{a}\frac{\cos\phi\,da}{[(x-a)^2+\eta^2]^m}=-\int_{-\infty}^{a}\frac{\rho\cos\phi\,d(x-a)}{[(x-a)^2+\eta^2]^m\rho}$$
$$=\int_{\rho_0}^{\infty}\frac{d\rho}{[(x-a)^2+\eta^2]^m}, \tag{A32}$$

where $\eta^2=y^2+(z-\tilde{z})^2/4$, and when $z=\tilde{z}$, $\eta^2=y^2$.

APPENDIX B. CALCULATION OF $F_{mn}(\tilde{\mathbf{r}}, \mathbf{r}, a)$

For calculating $H(\mathbf{r}, \tilde{\mathbf{r}})$ we need the integrals:

$$F_{mn}(\tilde{\mathbf{r}}, \mathbf{r}, a) = \int_{-\infty}^{\infty} [(\tilde{x}-a)^2 + (\tilde{y})^2 + (\tilde{z}-z')^2]^{-m}[(x-a)^2 + y^2 + (z-z')^2]^{-n}\,\mathrm{d}z'. \tag{B1}$$

where the position vectors $\tilde{\mathbf{r}} = (\tilde{x}, \tilde{y}, \tilde{z})$, $\mathbf{r} = (x, y, z)$ refer to the points on the surfaces of penny cracks. F_{11} can be obtained by using the method of residues

$$F_{11}(\tilde{\mathbf{r}}, \mathbf{r}, a) = \pi\left(\frac{1}{\rho} + \frac{1}{\tilde{\rho}}\right)F, \tag{B2}$$

where $F = [(z-\tilde{z})^2 + (\rho+\tilde{\rho})^2]^{-1}$, $\rho = \sqrt{(x-a)^2 + y^2}$ and $\tilde{\rho} = \sqrt{(\tilde{x}-a)^2 + \tilde{y}^2}$. The same method may also be used to evaluate all other F_{mn}. But a simpler way to do this is by using the recursive formulae:

$$\begin{aligned}
F_{m(n+1)}(\tilde{\mathbf{r}}, \mathbf{r}, a) &= -\frac{1}{2m\rho}\frac{\partial}{\partial \rho}F_{mn}(\tilde{\mathbf{r}}, \mathbf{r}, a),\\
F_{(m+1)n}(\tilde{\mathbf{r}}, \mathbf{r}, a) &= -\frac{1}{2m\rho}\frac{\partial}{\partial \tilde{\rho}}F_{mn}(\tilde{\mathbf{r}}, \mathbf{r}, a),\\
F_{(m+1)(n+1)}(\tilde{\mathbf{r}}, \mathbf{r}, a) &= -\frac{1}{4nm\tilde{\rho}\rho}\frac{\partial^2}{\partial \rho\,\partial \tilde{\rho}}F_{mn}(\tilde{\mathbf{r}}, \mathbf{r}, a).
\end{aligned} \tag{B3}$$

It is useful to know that the function F is symmetric with respect to ρ and $\tilde{\rho}$ and as far as this Appendix is concerned ρ and $\tilde{\rho}$ are independent. Symmetry with respect to ρ and $\tilde{\rho}$ is retained by all partial derivatives of F with respect to ρ or $\tilde{\rho}$, and the following relations hold among the derivatives:

$$\frac{\partial}{\partial \tilde{\rho}}\frac{\partial^{\alpha+\beta}F}{\partial \tilde{\rho}^{\beta}\,\partial \rho^{\alpha}} = \frac{\partial}{\partial \rho}\frac{\partial^{\alpha+\beta}F}{\partial \tilde{\rho}^{\beta}\,\partial \rho^{\alpha}} = \frac{\partial^{\alpha+\beta+1}F}{\partial \tilde{\rho}^{\beta+\alpha+1}} = \frac{\partial^{\alpha+\beta+1}F}{\partial \rho^{\beta+\alpha+1}}. \tag{B4}$$

By use of (B3) and the indicated symmetry properties of F and its derivatives, F_{mn} may be written as follows:

$$\begin{aligned}
F_{21} &= -\frac{\pi}{2\tilde{\rho}}\left[\frac{-1}{\tilde{\rho}^2}F + \left(\frac{1}{\rho} + \frac{1}{\tilde{\rho}}\right)\frac{\partial F}{\partial \rho}\right],\\
F_{22} &= \frac{\pi}{4\tilde{\rho}\rho}\left[-\left(\frac{1}{\rho^2} + \frac{1}{\tilde{\rho}^2}\right)\frac{\partial F}{\partial \rho} + \left(\frac{1}{\tilde{\rho}} + \frac{1}{\rho}\right)\frac{\partial^2 F}{\partial \rho^2}\right],\\
F_{31} &= +\frac{\pi}{8\tilde{\rho}^2}\left[\frac{3}{\tilde{\rho}^3}F - \left(\frac{1}{\tilde{\rho}\rho} + \frac{3}{\tilde{\rho}^2}\right)\frac{\partial F}{\partial \rho} + \left(\frac{1}{\rho} + \frac{1}{\tilde{\rho}}\right)\frac{\partial^2 F}{\partial \rho^2}\right],\\
F_{32} &= \frac{\pi}{16\tilde{\rho}\rho}\left[-\frac{1}{\tilde{\rho}^2}\left(\frac{1}{\rho^2} + \frac{3}{\tilde{\rho}}\right)\frac{\partial F}{\partial \rho} + \frac{1}{\rho}\left(\frac{1}{\tilde{\rho}\rho} + \frac{3}{\tilde{\rho}^2} + \frac{1}{\rho^2}\right)\frac{\partial^2 F}{\partial \rho^2} - \frac{1}{\tilde{\rho}}\left(\frac{1}{\rho} + \frac{1}{\tilde{\rho}}\right)\frac{\partial^3 F}{\partial \rho^3}\right],\\
F_{33} &= \frac{\pi}{64\tilde{\rho}\rho}\left[\frac{-3}{\tilde{\rho}^2\rho^2}\left(\frac{1}{\tilde{\rho}^2} + \frac{1}{\rho^2}\right)\frac{\partial F}{\partial \rho} + \frac{3}{\tilde{\rho}\rho}\left(\frac{1}{\tilde{\rho}^2\rho} + \frac{1}{\rho^2\tilde{\rho}} + \frac{1}{\rho^3} + \frac{1}{\tilde{\rho}^3}\right)\frac{\partial^2 F}{\partial \rho^2}\right.\\
&\quad \left. - \frac{1}{\tilde{\rho}\rho}\left(\frac{3}{\tilde{\rho}^2} + \frac{3}{\rho^2} + \frac{2}{\tilde{\rho}\rho}\right)\frac{\partial^3 F}{\partial \rho^3} + \frac{1}{\tilde{\rho}\rho}\left(\frac{1}{\tilde{\rho}} + \frac{1}{\rho}\right)\frac{\partial^4 F}{\partial \rho^4}\right].
\end{aligned} \tag{B5}$$

Moreover

$$\begin{aligned}
F_{12}(\tilde{\mathbf{r}}, \mathbf{r}, a) &= F_{21}(\mathbf{r}, \tilde{\mathbf{r}}, a),\\
F_{13}(\tilde{\mathbf{r}}, \mathbf{r}, a) &= F_{31}(\mathbf{r}, \tilde{\mathbf{r}}, a),\\
F_{23}(\tilde{\mathbf{r}}, \mathbf{r}, a) &= F_{32}(\mathbf{r}, \tilde{\mathbf{r}}, a).
\end{aligned} \tag{B6}$$

Derivatives of F may be written in terms of the powers of F:

$$\begin{aligned}
\frac{\partial F}{\partial \rho} &= -2(\rho+\tilde{\rho})F^2,\\
\frac{\partial^2 F}{\partial \rho^2} &= 6F^2 - 8(z-\tilde{z})^2F^3,\\
\frac{\partial^3 F}{\partial \rho^3} &= -24(\rho+\tilde{\rho})F^3 + 48(z-\tilde{z})^2(\rho+\tilde{\rho})F^4,
\end{aligned}$$

$$\frac{\partial^3 F}{\partial \rho^3} = 120F^3 - 96(z-\bar{z})^2F^4 - 384(z-\bar{z})^2(\rho+\bar{\rho})^2F^5, \tag{B7}$$

such that F_{mn} may finally be expressed as:

$$F_{21} = \pi\left[\left(\frac{1}{2\bar{\rho}^3} + \frac{1}{\rho\bar{\rho}^2}\right)F - \frac{1}{\rho\bar{\rho}^2}(z-\bar{z})^2F^2\right],$$

$$F_{22} = \frac{\pi}{2}\left[\left(\frac{1}{\rho} + \frac{1}{\bar{\rho}}\right)\left(\frac{3}{\bar{\rho}\rho} + \frac{1}{\rho^2} + \frac{1}{\bar{\rho}^2}\right)F^2 - 4(z-\bar{z})^2\frac{1}{\bar{\rho}\rho}\left(\frac{1}{\rho} + \frac{1}{\bar{\rho}}\right)F^3\right],$$

$$F_{31} = \frac{\pi}{8\bar{\rho}^2}\left[\frac{3}{\bar{\rho}^3}F + 8\left(\frac{1}{\bar{\rho}} + \frac{1}{\rho}\right)F^2 + 6\frac{\bar{\rho}+\rho}{\bar{\rho}^2}F^2 - 8\left(\frac{1}{\rho} + \frac{1}{\bar{\rho}}\right)(z-\bar{z})^2F^3\right],$$

$$F_{32} = \frac{\pi}{8\bar{\rho}}\left[\frac{1}{\bar{\rho}}\left(\frac{16}{\bar{\rho}\rho^2} + \frac{12}{\bar{\rho}^2\rho} + \frac{3}{\bar{\rho}^3} + \frac{4}{\rho^3}\right)F^2 - 4(z-\bar{z})^2\frac{1}{\bar{\rho}\rho}\left(\frac{4}{\bar{\rho}\rho} + \frac{1}{\rho^2} + \frac{3}{\bar{\rho}^2}\right)F^3 - 24(z-\bar{z})^2\left(\frac{1}{\rho} + \frac{1}{\bar{\rho}}\right)^2\right)F^4\right],$$

$$F_{33} = \frac{3\pi}{8}\left[\left(\frac{1}{\rho} + \frac{1}{\bar{\rho}}\right)\left(\frac{5}{\bar{\rho}\rho^3} + \frac{9}{\bar{\rho}^2\rho^2} + \frac{5}{\bar{\rho}^3\rho} + \frac{1}{\rho^4} + \frac{1}{\bar{\rho}^4}\right)F^3 - 2(z-\bar{z})^2\frac{1}{\bar{\rho}\rho}\left(\frac{1}{\rho} + \frac{1}{\bar{\rho}}\right)\left(\frac{4}{\bar{\rho}\rho} + \frac{3}{\rho^2} + \frac{3}{\bar{\rho}^2}\right)F^4 - 16(z-\bar{z})^2\left(\frac{1}{\rho} + \frac{1}{\bar{\rho}}\right)^3F^5\right]. \tag{B8}$$